Title
Assessment of seawater intrusion potential from sea level rise in coastal aquifers of California

Authors
Loáiciga, HA
Pingel, TJ

Publication Date
2008-12-01

Peer reviewed

Assessment of Seawater Intrusion Potential From Sea-level Rise in Coastal Aquifers of California

University of California Water Resources Center Technical Completion Report

Project SD017

By

Hugo A. Loáiciga
Department of Geography
University of California, Santa Barbara, CA 93106-4060
hugo@geog.ucsb.edu

Thomas J. Pingel
Department of Geography
University of California, Santa Barbara, CA 93106-4060
pingel@geog.ucsb.edu

Elizabeth S. Garcia
Department of Geography
University of California, Santa Barbara, CA 93106-4060
garcia@geog.ucsb.edu

December 1, 2009

Abstract

The California Department of Water Resources (2006) estimated a rise in mean sea level along California's coastline ranging from 10 to 90 cm over the 21st century due to rising global mean surface temperature. This range of sea-level rise is consistent with the Intergovernmental Panel for Climate Change (2007) estimates. The rise in sea level threatens coastal aquifers by exacerbating the risk of saline intrusion. This study simulated the effect of sea-level rise on the Seaside Area sub-basin near the City of Monterey, California. The simulation was carried out with a state-of-art, finite-element, variable-density, numerical model that accounts for the effects of salinity on groundwater density and viscosity. Seawater intrusion was simulated for various scenarios of sea-level rise, varying from 0 m to 1 m assuming a linear increase of sea level through the 21st century. Each scenario contemplated the same level of predicted groundwater extraction through the 21st century in the study aquifers. The numerical simulations of seawater intrusion indicate that one meter of sea-level rise would contribute an additional 10 to 15 meters of inland spread of the 1,000 mg/L saline front and 20 to 30 meters of the 10,000 mg/L saline front. The effect of sea-level rise on seawater intrusion in the Seaside Area sub-basin, therefore, appears minor when compared with historical measurements of seawater intrusion caused primarily by groundwater pumping since the early 1900s. Other aquifers with less topographical relief and more complex hydrostratigraphy could be more vulnerable to sea-level rise, however. One such possibility is posed by the Oxnard Plain groundwater sub-basin, in Ventura County, California. This study compiled a hydrogeologic database and structured the basic elements of a sea-water intrusion numerical simulation model for the Oxnard Plain aquifer. The Oxnard Plain sub-basin is a complex, multi-formation, aquifer that has undergone several decades of groundwater extraction, and, which is known to experience seawater intrusion in several of its coastal areas. The Oxnard Plain sub-basin features an important offshore hydrogeologic section that encompasses its boundary under seawater. Time limitations prevented calibration and validation of the numerical simulation model for seawater intrusion in the Oxnard Plain sub-basin. Nevertheless, the elements needed to complete the Oxnard Plain sub-basin's seawater-intrusion simulation model in the near future (with additional funding) have been assembled and are presented in this report. The approach presented in this report for the relatively assessment of groundwater extraction and sea-level rise effects on seawater intrusion into coastal aquifers holds potential for wide-ranging applicability in a variety of hydrogeologic settings. In particular, the finite-element spatial grid provides distinct capabilities to represent accurately the geographical layout of an aquifer.

1. Introduction: Problem Statement and Objectives

The California Department of Water Resources (CDWR) issued a landmark report in July 2006 describing progress made on incorporating climate change into management of California's Water Resources (CDWR, 2006). The CDWR identified saline intrusion into coastal aquifers as one likely impact of modern-age climate change. While sea-level has been rising since the end of the last (Wisconsinan) Ice Age, the rate of increase might have been recently exacerbated by thermal expansion and ice melting caused by anthropogenic greenhouse gas (GHG) emissions to the atmosphere (Intergovernmental

Panel for Climate Change –IPCC-, 2007). Other effects of increased GHGs emissions, CO_2, specifically, on seawater have been pondered in Loáiciga (2006, 2007).

Global mean sea-level (GMSL) increased by an average rate of 1.8 mm per year during the 20th century (Douglas, 1997) and the United Nations summary Panel on Climate Change (IPCC) reports a high confidence that this rate has been increasing (IPCC, 2007; Bates et al., 2008). The IPCC estimates that GMSL increased 3.1 mm/yr from 1993 to 2003, though this change is not spatially uniform worldwide. The eight long-term tidal records on the coast of California largely match the global trend with increases in mean sea level (MSL) ranging from 0.84 mm/yr (Los Angeles) to 2.22 mm/yr (La Jolla) and one station showing a decrease in MSL of -0.48 mm/yr (CDWR, 2006) during the 20th century.

The CDWR (2006) postulated an additional increase in sea-level ranging from 0.10 to 0.90 m along California's coast by 2100. One effect of such an increase in sea-level rise is to induce seawater intrusion into coastal aquifers (Zekster and Loáiciga, 1993; Werner and Simmons, 2009). Seawater intrusion has been noted in Monterey, Santa Cruz, and Ventura counties of California, and in lands surrounding the San Francisco Bay, dating back to the 1930s. Given the prominent role that groundwater has on water supply in California – amounting to about 30% of its urban and agricultural water use – it is timely to address the threat posed by future sea-level rise to California's groundwater.

While seawater intrusion into coastal aquifers is a long-studied problem (Ghyben, 1888; Herzberg, 1901) the relatively recent development of powerful numerical models has enabled in-depth three-dimensional modeling of freshwater-seawater interactions at specific sites (Yeh and Bray, 2006; Bray et al., 2007; Kumar et al., 2007). The papers by Giambastiani et al. (2007) and Masterston et al. (2007) considered sea level rise effects during the 21st century on seawater intrusion. FEFLOW is one such numerical modeling software system capable of accounting for density-dependent solute-transport (Diersch, 2006; Trefrey and Muffels, 2007) and thus, appropriate for simulating seawater intrusion in coastal aquifers caused by natural and anthropogenic processes. There have been several recent uses of FEFLOW to model seawater intrusion into coastal aquifers. Faye et al. (2001) modeled sea-water intrusion into a confined aquifer in Senegal. Kumar et al. (2007) modeled sea-water intrusion using a seven-layer FEFLOW model. Barazzuoli et al. (2008) used FEFLOW to model seawater intrusion caused by pumping near coastal production wells. An exhaustive literature review of sea-level rise and seawater intrusion is beyond the scope of this work.

This report summarizes a numerical simulation of seawater intrusion into a coastal aquifer by the combined effects of secular rise in sea-level rise and groundwater extraction. Seawater intrusion was modeled in this study at the Seaside Area Sub- basin of the Salinas Valley Groundwater Basin (No. 3-4.08, according to numbering scheme by the CDWR, 2003). The Seaside sub-basin features relatively high topographic relief, steep groundwater gradients, unconfined flow, and relatively simple stratigraphy with approximately homogeneous hydraulic conductivity (Muir, 1982). The tidal monitoring station in the City of Monterey shows an average annual sea-level rise of 1.34 mm based on online data from 1973 to 2006 (National Oceanic and Atmospheric Administration – NOAA- 2009). In addition, this project initiated the research to structure a numerical simulation model for the Oxnard Plain ground-water sub-basin, in Ventura County, California. Specifically, this work compiled a hydrogeologic database and structured the basic elements of a sea-water intrusion numerical simulation model for the Oxnard Plain sub-basin. The Oxnard Plain sub-basin is a complex, multi-formation (i.e., multi-layer), aquifer that has undergone several decades of groundwater extraction, and which is known to experience seawater intrusion in several of its coastal areas. The Oxnard Plain sub-basin features an important offshore hydrogeologic section that encompasses its boundary under seawater. Time limitations prevented calibration and validation of the numerical simulation model for seawater intrusion in the Oxnard Plain sub-basin. Nevertheless, the elements needed to complete the Oxnard Plain sub-basin's seawater-intrusion simulation model with additional funding in the near future have been assembled and are presented in this report. The approach presented in this report for the relatively assessment of groundwater extraction and sea-level rise effects on seawater intrusion into coastal aquifers holds potential for wide-ranging applicability in a variety of hydrogeologic settings.

2. Site Description: the Seaside Area Sub-basin

The Seaside Area sub-basin (3-4.08) is part of the large Salinas Valley Groundwater Basin of Monterey County, California. The sub-basin is approximately 10,500 hectares in area. The hydrogeologic setting of the Seaside Area sub-basin was described in detail by Muir (1982). Figure 1 shows a location map for the Seaside Area sub-basin. See section 2.3 for a brief hydrogeologic description of the Seaside Area sub-basin.

The coastal area receives approximately 43 cm of rain per year, while the inland areas receive approximately 38 cm of rain per year (CDWR, 2003). The subbasin lies northwest/southeast with groundwater generally flowing from the southeastern foothills (150 to 250 meters in elevation near the subbasin boundary) to the sea. The urban area connected to the city of Seaside is largely concentrated near the southern portion of the coastal section. According to census figures, the city of Seaside has (as of 2007) a population of some 33,500 people, a number largely unchanged since 1990.

The bulk of the sub-basin is occupied by the Fort Ord Military Reservation, which closed as an active duty base in 1994. As a result, the greater area of the sub-basin is undeveloped with the exception of several ranches along the southern border. There are only a few small streams within the basin, with most surface drainage occurring into small depressions (CDWR, 2003). Vegetation is generally coastal scrub and chaparral throughout the area (Yates et al., 2005).

2.1 Groundwater Interactions

Yates et al. (2005) report that while there are 20 active wells in the sub-basin, nearly all water (99%) comes from only thirteen of these wells. These wells are spatially concentrated within 3 kilometers of the coast. While Muir (1982) reported an average annual groundwater extraction of 4.44×10^6 m^3 (3,600 acre-feet/yr), the average annual extraction from 1995 to 2005 was 5.5×10^6 m^3 (4,500 acre-feet/yr). Figure 2 shows the increase in total production from the twenty historically most active wells since 1956 (assembled from historical data presented by Durbin, 2007). Yates et al. (2005) calculated the mean total extraction for 2000 to 2006 as approximately 6.88×10^6 m^3/yr (5,600 acre-feet/yr).

Contention over groundwater pumping between commercial, municipal and private users led to a Court-appointed Water Master for the Seaside Area groundwater sub-basin. The Water Master is tasked with acting as arbiter between all parties and setting limits on groundwater extraction. Decreasing groundwater levels (Muir, 1982; Yates et al., 2005; Durbin, 2007), particularly a below-sea-level depression near the coastal production wells, caused the Court to mandate that extraction must decrease annually until the operating yield is less than the sustainable yield. Figure 2 shows the spatial location of the current extraction, while Figure 3 shows extraction from the twenty principal wells since 1956. Most water extracted is for urban use, though some is used for agriculture and golf courses (CDWR, 2003).

Yates et al. (2005) estimated the total sustainable (annual) yield at 3.55 x 10^6 m^3 (2,880 acre-feet/yr), though "substantial uncertainty" surrounds this estimate. The extraction imbalance, or overdraft, whereby groundwater pumping exceeds recharge, has been mitigated to some extent by the introduction of two injection wells near the coast. These two wells accounted for just over 600 m^3/d of water injected. However, groundwater levels near the coast have been in steady decline since at least 1982 (Muir, 1982) at a rate of 0.2 m to 0.3 m (0.7 to 1.0 ft) per year (Yates et al., 2005). There is currently a cone of depression of some 3 to 6 meters (depending on the season) surrounding the largest production wells about 2.5 km from the coast.

2.2 Hydrogeology

The study area has three main water-bearing structures bounded by shale on the bottom (Muir, 1982; Yates et al., 2005). The bottommost layer is the Santa Margarita Formation and consists of poorly consolidated marine sandstone. On top of this lies the Paso Robles Formation, which is also largely sandstone with some clay and gravel. Overlaid on the Paso Robles Formation are dune sand deposits in some areas. A sometimes-mentioned fourth structure, the Aromas Formation, is typically grouped with either the Paso Robles or dune sand deposits due to similarity in structure. There is no barrier to flow between these units (Muir, 1982), and all share very similar average hydraulic conductivity values. The aquifer system thickness varies, with some locations exceeding 300 meters. In general, the aquifer system is thickest to the north, and thins substantially toward the south. Hydraulic conductivity estimates, however, vary. Fugro West Inc.'s (1997) report empirically derived hydraulic conductivity estimates in the range of 6 to 18 m/d throughout the basin, while Yates et al, (2005) estimated approximately 0.5 to 1.5 m/d based on numerical model calibrations.

3. Description of the Numerical Seawater-Intrusion Model for the Seaside Area Sub-basin

A three-dimensional, finite-element, model of the Seaside Area sub-basin was constructed using the FEFLOW software package, version 5.3 (Diersch, 2006). Three scenarios of sea-level rise were used to simulate seawater intrusion: 0.0, 0.5 and 1.0 m rise over the period 2006-2106. Each scenario assumes current groundwater extraction continues into the future, as suggested by the existing trends of groundwater extraction in this sub-basin. The assumed groundwater extraction equals the five-year average of the principal extraction wells from 2002 to 2006, and equaled 5.6 x 10^6 m^3/yr.

FEFLOW is a numerical, coupled, groundwater flow-solute transport-heat numerical simulation model. This study assumed isothermal flow, thus bypassing the need for simulating heat transport. FEFLOW uses a finite-element spatial grid, giving it unique capabilities to represent accurately the geographical layout of an aquifer. Figure 4 shows a plan view of the finite-element mesh for the Seaside Area sub-basin. The model allows time-dependent and spatially variable recharge, pumping, injection, and boundary conditions. The mathematical equations of flow and solute transport solved by FEFLOW in this study (after discretization in a finite-element grid) are:

Groundwater flow equation (Diersch, 2006; see, also, Langevin and Guo, 2006):

$$\nabla \cdot \left[\rho K \left(\nabla h + \frac{\rho - \rho_W}{\rho_W} \nabla z \right) \right] = \rho S \frac{\partial h}{\partial t} + \phi \frac{\partial \rho}{\partial C} \frac{\partial C}{\partial t} \qquad (1)$$

in which ρ = density of saline groundwater; ρ_W = the density of fresh groundwater (approximately 1,000 kg/m^3); z = elevation head; ϕ = porosity; S = specific storage; C = the concentration of dissolved solids (or salinity) in groundwater; h = freshwater equivalent hydraulic head, which is equal to the elevation head plus the pore-pressure head of groundwater scaled by the ratio ρ / ρ_W; t = the time variable; ∇ = the gradient operator in three dimensional, Cartesian, coordinates; K = hydraulic conductivity, where K = $k \rho g / \mu$, k = permeability, g = acceleration of gravity, and μ = dynamic viscosity.

Solute transport equation (Diersch, 2006; see, also, Langevin and Guo, 2006):

$$\frac{\partial \phi C}{\partial t} = \nabla \cdot \left(\phi D \cdot \nabla C \right) - \nabla \cdot \left(q C \right) \qquad (2)$$

in which D = hydrodynamic dispersion tensor, q = Darcian flux of groundwater, all other variables defined after equation (1).

In addition, there are empirical equations relating the density ρ and (dynamic) viscosity μ to salinity, pore pressure, and water temperature (see Diersch, 2006). Equations (1) and (2), together with the empirical equations for density and viscosity are discretized via the finite-element method and solved numerically in FEFLOW (see Diersch, 2006).

3.1 Elevation datums, Coordinate Systems, and Units

Most of the existing geographical data used were originally in the State of California Plane Coordinate System (California Zone IV), and used the National Geodetic Vertical Datum of 1929 (NGVD29) and the North American Datum of 1927. These were reprojected into the Universal Transverse Mercator (Zone 11N) coordinate system, North American Vertical Datum of 1988 (NAVD88), and the World Geodetic System of 1984. Data were also typically provided in the US customary system of units and were converted to their respective metric values. Since the impact of MSL was a principal variable of interest for this study, it was crucial to accurately relate the various vertical datums (e.g., mean sea level and its near-approximations) at the coast. NOAA provides online data calculated from coastal benchmarks. According to these data, for the epoch 1983-2001, the vertical datums are related as shown in Table 1 (National Geodetic Survey, 2009).

The "zero" mark for our models corresponded to the NAVD88 datum. As a result, year 2006 sea level was modeled as 0.903 meters above this datum. Table 1 also shows tidal variation between the mean highest daily tide and lowest daily tide. This variation is approximately 1.63 meters.

3.2 Model Boundaries and Finite-Element Mesh.

Model boundaries of the Seaside Area sub-basin were initially well-defined by Muir (1982) and refined by Yates et. al (2005). These outer boundaries were supplied to the authors by the Monterrey Peninsula Water Management District (Sandoval, 2008). The total size of the basin, as modeled, was 6038 hectares. The southwest boundary was derived from the Chupines fault location where uplifted Monterey shale formation prevents groundwater from flowing. The eastern boundary results from a flow divergent pattern defined by topography. Each of these was included in the model as no-flow boundaries. The northeast boundary is largely administrative since flow is in the direction of the boundary. It was also modeled as a no-flow boundary. The boundary itself is a relative high head area between pumping zones of Seaside to the southwest and Salinas to the northeast. Interior boundaries are divisions based on patterns of topography, soil type and land cover based on Yates et al. (2005).

It was stated in sub-section 2.1 that there are four formation units described in the aquifer system (Muir, 1982; Yates et al., 2005). The surface of the top layer was generated from the National Elevation Dataset at a resolution of one arc second (USGS, 2008). The position of the bottom (shale) layer was estimated from cross-sections presented in Muir (1982) and Yates et al. (2005). These cross sections were scanned, and geo-referenced, and the resulting lower surface was then interpolated and extrapolated using the Matlab implementation of Sandwell's biharmonic spline algorithm (Sandwell, 1987).

Due to differences in land cover, land use, and rainfall, Yates et al. (2005) divided the Seaside sub-basin into four sub-areas, the division of which can be seen in Figure 3. Nearly all groundwater in the sub-basin is extracted from the northern coastal subarea, and no groundwater is extracted from the northern inland subarea. The authors used these four areas to model hydraulic conductivity, storage coefficient, and net groundwater inflow within the aquifer, following the approach of Yates et al. (2005).

The FEFLOW model utilized a triangular mesh consisting of approximately 10,000 nodes. The nodes were initially set rather coarsely, but were later refined near the coast and wells to improve numerical accuracy by enhanced spatial resolution near these features, as per guidelines in FEFLOW documentation (Diersch, 2006), as shown in Figure 4.

It is possible that sea-level rise impacting unconfined aquifers with low topographic relief rise could change the sea-side boundary significantly enough to require a corresponding accommodation in the shape of the numerical model. However, in the Seaside Area sub-basin, this paper's analysis showed that even the maximum one-meter change in sea level did not substantially modify the shape or location of the shoreline.

3.3 Boundary Conditions and Parameters

The ocean boundary of the model was assigned a head of 0.903 meters (MSL for present epoch in local reference to the NAVD88 vertical datum) for 2006, and a total dissolved solid content (or salinity of average seawater) equal to 35,000 ppm, or approximately equal to 35,000 mg/L. The sea level on the coastline was increased linearly over the 100-year modeling period to reach a specified total rise at the end of the period.

The twenty-two wells referred to in section 2.1 were used to model extraction and injection for the sub-basin. Twenty of these were extraction wells. The other two were injection wells. The locations and extraction amounts were taken from Durbin (2007) and corroborated with Yates et al. (2005). Each five-year period was averaged and entered in FEFLOW as a dynamic pumping well. Extraction for the 2002-2006 period averaged 16,007 m^3/d. Additionally, the two test injection wells were also included for their years of operation, and into the future, through 2106. Together, these two wells accounted for an average injection of 628 m^3/d.

Net top inflow (recharge) was assigned the following values for each sub-area (in mm/d): Northern Coastal = 0.401, Southern Coastal = 0.309, Northern Inland = 0.175, Southern Inland (Laguna Seca) = 0.223. The overall spatially weighted mean recharge for the sub-basin was 0.231 (or 28 feet/year), which is close to the value used by Durbin (2007).

Horizontal conductivity (K_{xy}) was assigned an initial value of .08 x 10^{-4} m/s. Vertical conductivity (K_z) was assigned an initial value of .035 x 10^{-4} m/s. These estimates underwent calibration to yield final values of hydraulic conductivity that were largely in line with those published by Yates et al. (2005). K_z was assigned a value equal to half of calibrated K_{xy}, since Muir (1982) reported partial confinement due to differences in vertical conductivity (CDWR, 2003). Storativity was ultimately assigned a value of 0.12 after calibration. This is higher than the value reported in Yates et al. (2005) but consistent with other work (Muir, 1982). Longitudinal and transversal dispersivities were assigned typical values for lithologies comparable to those found in the study aquifer. These values were selected from a database from Waterloo Hydrogeologic Inc. (2000) and performed well in calibrating the FEFLOW numerical simulation model.

4. Calibration of the Numerical Model and Simulation Results for the Seaside Area Sub-basin

The calibration phase for the Seaside numerical simulation model consisted of two phases. The first phase (pre-calibration) involved systematically varying the principal parameters: net inflow (recharge), storativity, and hydraulic conductivity until an acceptable water-table gradient was found that roughly matched pre-extraction hydraulic head data. These data are often incomplete. Based on accounts reported in Muir (1982), an average hydraulic head gradient of approximately 0.008 was assumed in this study to reconstruct pre-extraction hydraulic head, given Muir's identification of 100 meter head near Laguna Seca, about 12 km inland.

The second calibration period consisted of simulating the period 1956-2006. The five-year average pumping yields described in section 3.3 served as the basis for well extraction and injection values. During this phase, an attempt was made to meet three criteria. First, overall water levels were allowed to drop until they approximately matched the contours published in Muir (1982) and Yates et al. (2005) for 1979 and 2002, respectively. Second, the hydraulic head simulations were refined to replicate the cone of depression of a size and depth nearly equal to the one that currently surrounds the production wells in the northern coastal subarea. Third, the calibration simulations were refined so that no appreciable seawater intrusion occurred by the year 2006, consistent with field conditions. These criteria were met in the final calibrated model.

The single largest driver to seawater intrusion into the Seaside area sub-basin is the balance between groundwater extraction rate and recharge into the aquifer system. Figure 5 shows the estimated head distribution for year 2106 based on year 2006 pumping rates and no change in sea-level from the present day. The depression that currently exists around the major production wells deepens and the overall gradient becomes landward.

Simulations for year 2106 reached very similar results with regards to overall head levels and sea-water intrusion. In all three scenarios of sea-level rise (that is, 0, 0.5, and 1.0 m secular rise), the 10,000 mg/L saline front lies 600 to 700 meters inland in the area near the production wells, while the 1,000 mg/L front intruded 1.0 to 1.2 kilometers in the same area. Figure 6 illustrates the total saline intrusion for year 2106 assuming 1 meter of sea level rise.

Figure 7 illustrates the differences between the scenarios in saline front location in year 2106. The scenarios that modeled a rise in sea level had saline fronts farther inland than the scenarios with no sea level rise. The difference in travel distance was larger for higher saline concentrations. The 10,000 mg/L front was located approximately 20 to 30 meters further inland for the one meter sea-level rise scenario than the front for the zero meter sea-level rise scenario. The 1,000 mg/L front was located approximately 10 to 15 meters inland. Evidently, given the large difference between 2006 groundwater extraction rates and the sustainable yield – the former being larger - the relative impact of sea-level rise on the system is small. In the Seaside Area sub-basin, groundwater extraction dominates over the range of sea-level rise considered.

5. Discussion of Results for the Seaside Area Sub-basin

This research attempted to quantify what effect sea-level rise will have on saline intrusion into coastal aquifers. Based on the results of the Seaside Area sub-basin model, seawater intrusion due to sea-level rise is a concern secondary to controlling groundwater extraction. The numerical model indicates an expanded zone of seawater intrusion of 10 to 30 meters approaching the coastal production wells given 1 m of sea-level rise over the next 100 years. Given the nearly one kilometer of net spread estimated over the course of the simulation period and the uncertainty inherent in the extraction regime in the subbasin over this length of time, the calculated effects of sea level rise appear secondary in the test aquifer. Other aquifers may show greater vulnerability to sea-level rise. This is a topic of continuing research whose results will be reported at a later time.

The methodology presented here used mean annual inputs rather than accounting for seasonal variability. Water tables in California are, in fact, highly subject to seasonal variability. It is not uncommon for head to fluctuate more than 5 to 8 meters between the end of the dry season (fall) and the end of the wet season (winter). Additionally, we did not account for the effect of tidal variation. While much more regular, and of a lower amplitude than the freshwater elevation changes, tidal variation in these two sub-areas is in excess of 1.5 meters. Each of these fluctuations would tend to widen the mixing zone. Additionally, severe seasonal variability (e.g., prolonged drought) could cause episodic large-scale seawater intrusion whose effects may take decades to fully abate.

Werner and Simmons (2009) recently conducted a meta-analysis of numerical simulations of sea-level driven coastal seawater intrusion and found that the type of landward boundary condition (flux controlled versus head controlled) contributed greatly to the horizontal extent of seawater intrusion observed. In our case, the landward boundaries for Seaside were flow-based and therefore, according to Werner and Simmons's results, ought to predict a lesser amount of saline intrusion that would a model utilizing landward head-based boundary conditions.

6. Site Description: the Oxnard Plain Sub-basin, Ventura County, California.

The Oxnard Plain sub-basin is part of the Santa Clara River Valley Groundwater Basin (numbered 4-4.02 by CDWR, 2003). It is nearly twice the size of the Seaside study area, totaling 23,500 hectares (58,000 acres, 90.6 square miles) (CDWR, 2003). Most of the sub-basin is of very low relief. The surface of the sub-basin ranges in slope from 0.3 percent in the northeast to 0.1 percent in the southeast. In other respects – land cover, average annual rainfall, and streamflow – the sub-basin is quite similar to the Seaside Area sub-basin. The population of the City of Oxnard is currently (2007) estimated at nearly 185,000 people, a number substantially larger than that in 1990 (142,000). The Oxnard sub-basin's groundwater is also heavily mined for agricultural use. The Oxnard sub-basin is hydraulically separated from the neighboring Santa Clara River Valley (to the north) by the Oak Ridge Fault. It is hydraulically connected to the Pleasant Valley sub-basin, and pumping in the Pleasant Valley sub-basin creates water table gradients that tend to cause northeasterly flows (from Oxnard to Pleasant Valley) in the northern part of the Oxnard sub-basin. Figure 8 shows the Oxnard sub-basin and adjacent sub-basin of the Santa Clara River Valley hydrologic system.

6.1 Groundwater Interactions

Hanson et al. (2003) estimated the pre-development groundwater hydraulic head near the coast was 12 to 15 m higher than the ground surface, based on accounts of artesian wells in the area. The advent of year-round farming in the 1940s significantly contributed to groundwater extraction, and, today, agriculture still accounts for most of the use of groundwater and surface water in the Oxnard area.

Groundwater extraction exceeds recharge in the Oxnard sub-basin, which has created a condition of chronic overdraft. The aquifer system in the Oxnard sub-basin held approximately 6,636 x 10^6 m^3 (5,380,000 acre-feet) of water in storage in 1999. Annual extraction was 80.18 x 10^6 m^3 (65,000 acre-feet), with recharge estimated at 12.58 x 10^6 m^3 (10,200 acre-feet) per year (CDWR, 2003). Though water levels remain largely stable in the sub-basin as a whole, parts of the southern sub-basin near Point Mugu and in the northernmost area near the Pleasant Valley subbasin continue to decline (Bachman and Detmer, 2004). Analysis of hydrographs in the area shows wide (25 m) fluctuations in water levels since 1975. In the early 200s hydraulic levels were in the upper range, at roughly 75% of those occurring at full capacity (CDWR, 2003).

6.2 Hydrogeology

The hydrogeology of the Oxnard Plain sub-basin is substantially more complex than that of the Seaside Area sub-basin. Five geologically distinct aquifers comprise the system (CDWR, 2003; Hanson et al., 2003; Bachman and Detmer, 2004). The bottommost are the Fox Canyon and Hueneme aquifers. These are separated by a thin, clay layer (or aquitard), and together comprise the Lower Aquifer System (LAS) for the basin. The Mugu and Oxnard aquifers together comprise the Upper Aquifer System (UAS), though these are also separated from each other and the LAS by clay layers (or aquitards). On top of these rest one more clay layer and a semi-perched zone of largely unusable unconfined groundwater. The many clay layers prevent direct vertical recharge, but discontinuities in the confining layers in the northwest part of the sub-basin, the Oxnard Forebay area, allow recharge.

7. Description of a Preliminary Numerical Seawater-Intrusion Model for the Oxnard Plain Sub-basin.

7.1 Overview

A three-dimensional finite element model of the Oxnard Plain subbasin was constructed using the FEFLOW software package, version 5.3 (Diersch, 2006). An overview of FEFLOW was given in Section 3. Due to the high level of hydraulic connection with the Oxnard Plain sub-basin, the neighboring Pleasant Valley sub-basin was included in the numerical simulation model FEFLOW as well.

7.2 Datums, Coordinate Systems, and Units

Most of the existing sea-level and terrain elevation data provided by various agencies were in the State Plane Coordinate System (California Zone V), and used the National Vertical Datum of 1929 and the North American Datum of 1927. These data were re-projected into the Universal Transverse Mercator (Zone 11N) coordinate system, North American Vertical Datum of 1988, and the World Geodetic System of 1984. Data were also typically provided in English units and were converted to their respective metric values. Table 2 shows the relationships for vertical datums at the nearest land-based station to the Oxnard Plain sub-basin.

7.3 Aquifer Layers

Several existing data sets provided the hydrogeological basis for the model. David Panaro (personal communication, 2008, Staff Geologist of the Fox Canyon Groundwater Management Agency) and Dan Detmer (personal communication, 2008, Senior Hydrologist of the United Water Conservation District) provided identical data sets of the relevant hydrogeology. These included six layers detailing the elevations of: the Lower Aquifer system's bottom and top surfaces (Fox Canyon and Hueneme aquifers), the Mugu Aquifer (bottom and top), and the Oxnard Aquifer (bottom and top surfaces). A unified surface elevation and bathymetry data layer from the National Geophysical Data Center provided the spatial location of the surface layer and seaward boundary for the aquifer system.

7.4 Model Boundaries

While the Oxnard Plain sub-basin was the intended focus, hydraulic interconnections among neighboring sub-basins necessitated their inclusion as well. The numerical simulation model was defined by UTM eastings (281100, 320140) and northings (3770100, 3793400), for zone 11. Although the Oxnard Plain sub-basin ends just north of the Mugu submarine canyon, recent studies indicate that the aquifer layers extend underwater three to four kilometers southeast of this point (Hanson et al., 2003). Pumping in the Lower Aquifer System in the (adjacent) Pleasant Valley sub-basin necessitated its inclusion into the numerical simulation model for the Oxnard Plain sub-basin. However, the neighboring Mound sub-basin was not included, since the Oak Ridge Fault was believed to act as a restrictive feature to flow (Panaro, 2008, personal communication). The boundary between the Oxnard Plain sub-basin and the Mound and Santa Paula groundwater basins is perpendicular to the groundwater-elevation contours in both the upper and lower aquifer layers, lending credibility to the model cutoff point at this location. In the numerical model, this is represented as a no-flow boundary. A no-flow boundary is appropriate since the boundary is parallel to the groundwater flow, and thus, there is no net interchange of water across the boundary.

A key feature of the Oxnard Plain numerical simulation model is the inclusion of offshore boundaries. The Seaside Area sub-basin boundaries, on the contrary, were coincident with the shoreline. However, the principal aquifers used for groundwater extraction on the Oxnard Plain are confined and remain so for several kilometers seaward. As a result, the initial pre-development saltwater interface is unknown. While Bachman and Detmer (2004) assess the most currently known seawater intrusion near the Hueneme and Mugu submarine canyons, the extent, concentration, and rate of intrusion through the offshore portion of the aquifer are entirely unknown.

Onshore, the depths of aquifers and separating clay layers were bi-cubically interpolated from digital elevation contours of each layer provided by the Fox Canyon Groundwater Management Agency (FCGMA). Each aquifer was defined separately, with the exception of the Lower Aquifer System (Fox Canyon and Hueneme aquifers), which was modeled as a single unit. To extend the boundaries offshore, we used a nearest-neighbor geometric extrapolation in the areas outward from the shoreline. This allowed each layer to repeat its vertical dimension longitudinally from the coast in a seaward direction. These extensions were then paired with a 1 arc second resolution coupled bathymetry / elevation layer from the Southern California Coastal Ocean Observing System (SCCOOS, 2009) to create a three-dimensional offshore geometric representation of the aquifer system. Figure 9 shows the final offshore and onshore boundaries of the Oxnard Plain / Pleasant Valley model. Figure 10 shows a sample onshore/offshore transect running through the Hueneme submarine canyon. The top black line represents the elevation of the land surface, both above and below sea-level.

FEFLOW has two limitations on the arrangement of layers that make it difficult to model offshore confined aquifers. Layers in FEFLOW must cover the entire span of the model, and layers must not intersect. Since the top geometric boundary of the uppermost layer of the model is the land surface, the uppermost layer begins to intersect with layers in the offshore portions of the model. From this intersection to seaward, the digital representation of the model cannot faithfully represent the true physical structure. The requirement that each layer have the same spatial extent requires that the end of the model terminate in a steep "cliff face." In unconfined aquifer cases (as in the Seaside sub-basin) this is not a problem, since the mixing zone will always be landward of the shoreline due to differences in seawater density as compared to freshwater. However, in cases of confined aquifers, the interface (under predevelopment conditions) is significantly seaward. In the model presented above, the seaward boundary was fixed at the top of the Oxnard aquifer. This should provide a correct model for seawater intrusion in the Oxnard aquifer, but not for the Mugu aquifer or the Lower Aquifer System.

There are two approaches in accommodating the layer-extent limitations in FEFLOW. The first method entails extending the layers at the thickness they have when they reach the land-ocean boundary. Seaward of the point of intersection, they are assigned high conductivity values and constant head and mass consistent with seawater. This would result in each layer having a relatively high number of boundary conditions (since each node in an area occupied by the sea would have a boundary condition). It would also tend to simplify the shape of the sea-land interface, creating a "cliff-face" structure at the intersection of each layer.

A second approach entails allowing each layer to follow a minimum set distance (i.e., 1 mm) above the layer beneath it seaward from the sea-land interface. The area of each layer corresponding to the sea is, as in the previous method, assigned a high conductivity value. However only the top layer is assigned a constant head and mass boundary consistent with seawater. This approach has the advantage of more correctly preserving the shape of each layer's sea-land interface as there is no steep "cliff-face" to mark the boundary. It also reduces the computational complexity by having markedly fewer boundary conditions in the simulation.

At the conclusion of the project, we compared each of these two approaches in simplified contexts. Both produced correct results for highly simplified systems, though the reduction in the number of boundary conditions in the second method improved solution times. At the conclusion of the study, we were in the process of testing this approach on a simplified three-dimensional model of the Hueneme submarine canyon offshore area. Future work will attempt to complete the numerical seawater simulation model for the Oxnard Plain sub-basin.

7.5 Freshwater-Saltwater Boundary

Given the general lowering of the water table in the Oxnard area from predevelopment conditions, it is likely that the freshwater-seawater interface is significantly landward from its predevelopment location. The report by Bachman and Detmer (2004) corroborates this conjecture. Correctly approximating the landward movement of the seawater boundary over time is crucial to estimating current conditions, and, particularly, in simulating future conditions. The principal effort during the closing months of the project involved assessing the transition zone in the upper and lower aquifer systems. Since the Heuneme and Mugu submarine canyons cut into the continental shelf, they are the most likely sources of initial seawater intrusion. The authors constructed several vertical cross-sectional models slicing, in a offshore-onshore orientation, through the Hueneme canyon and specified freshwater heads consistent with predevelopment and current conditions. This set of vertical slices served as the starting point for the final calibration of the entire three-dimensional model. The final model was not completed due to the complexities of the offshore aquifer systems and limitations in FEFLOW described above.

8. CONCLUSION

In the Seaside Area sub-basin, unconfined coastal aquifer system, we estimate that a sea-level rise of one meter over one hundred years will cause an additional 10 to 30 meters of horizontal spread of saline water. Steep hydraulic gradients towards the sea in the unconfined aquifer of this sub-basin abate seawater intrusion for the given groundwater extraction rates. The case of seawater intrusion into the Oxnard Plain sub-area proved substantially more difficult to simulate, due to the much-increased complexity of its hydrostratigraphy and the lack of information concerning the spatio-temporal advance of the saline front through the offshore portion of the aquifer system. Our future work entails developing approximate ways to model the presence of an underwater portion of the Oxnard Plain sub-basin and complete a fully coupled (flow-saline transport) numerical simulation model for this aquifer system.

The results of this project indicate the feasibility of implementing a state-of-the-art numerical simulation model like FEFLOW to simulate coupled groundwater flow and seawater intrusion due to the combined effects of groundwater pumping and sea-level rise. The case of aquifer systems extending offshore, however, presents complications that are still under research to achieve satisfactory resolution.

Acknowledgements

This project was made possible through grant SD017 from the University of California Water Resources Center. The authors also wish to thank management officials at the Monterey Peninsula Water Management District, the Fox Canyon Groundwater Management Agency, and the United Water Conservation District for their invaluable assistance in acquiring digital data for the study areas and for providing clarifications and interpretations of existing reports on groundwater in their respective basins.

Bibliography

Bachman, S., and D. Detmer. 2004. 2003 Coastal Saline Intrusion Report, Oxnard Plain, Ventura County, California, 25: Groundwater Resources Department, United Water Conservation District.

Barazzuoli, P., M. Nocchi, R. Rigati, and M. Salleolini. (2008). A conceptual and numerical model for groundwater management: a case study on a coastal aquifer in southern Tuscany, Italy. *Hydrogeology Journal* 16 (8):1557-1576.

Bates, B., Z. W. Kundzewicz, S. Wu, and J. Palutikof, eds. (2008). *Climate Change and Water. Techincal Paper of the Intergovernmental Panel on Climate Change*. Geneva: IPCC Secretariat.

Bray, B., F. T. Tsai, Y. Sim, and W. W. Yeh. (2007). Model Development and Calibration of a Saltwater Intrusion Model in Southern California. *Journal of American Water Resources Association* 43 (5):1329-1343.

California Department of Water Resources (CDWR). (2003). California's Groundwater.

Bulletin 118. Sacramento, California.

California Department of Water Resources (CDWR). (2006). Progress on Incorporating Climate Change into Management of California's Water Resources. Sacramento, California.

Detmer, D. 2008. Senior Hydrologist, United Water Conservation District. Written communication, January 18, 2009.

Diersch, H. J. G. (2006). *FEFLOW 5.3: Finite Element Subsurface Flow and Transport Simulation System User Manual Version 5.3*. Berlin: WASY GmbH Institute for Water Resources Planning and Systems Research.

Douglas, B. C. (1997). Global Sea Level Rise: A Redetermination. *Surveys In Geophysics* 18 (2-3):279-292.

Durbin, T. J. (2007). Groundwater Flow and Transport Model: Seaside Groundwater Basin, Monterey County, California, 33: RBF Consulting.

Faye, S., I. N. Diop, S. C. Faye, D. G. Evans, M. Pfister, P. Maloszewski, and K. P. Seiler. (2001). Seawater intrusion in the Dakar (Senegal) confined aquifer: calibration and testing of a 3D finite element model. In *New Approaches Characterizing Groundwater Flow*, eds. K. P. Seiler and S. Wohnlich, 1183-1186: Swets & Zeitlinger Lisse.

Fetter, C. W. (2001). *Applied Hydrogeology*. 4th ed. Upper Saddle River, N.J.: Prentice Hall.

Fugro West Inc. (1997). Hydrogeologic Assessment, Seaside Coastal Groundwater Subareas, Phase III Update. Monterey County, CA: MPWMD.

Ghyben, B. W. (1888). Nota in verband met de voorgenomen putboring nabij Amsterdam (Notes on the probable results of the proposed well drilling near Amsterdam), 8–22. The Hague: Tijdschrift van het Koninklijk Institunt van Ingeniers.

Giambastiani, B., Antonellini, M., Oude Essink, G.H.P., Stuurman, R.J. (2007). Saltwater intrusion in the unconfined coastal aquifer of Ravenna (Italy): a numerical model. *Journal of Hydrology,* 340(1-2):91-104.

Hanson, R. T., P. Martin, and K. M. Koczot. (2003). Simulation of Ground-Water/Surface-Water Flow in the Santa Clara-Calleguas Basin, Ventura County, California. Sacramento, California: U.S. Geological Survey.

Herzberg, A. (1901). Die Wasserversorgung einiger Nordseeb~ider (The water supply on parts of the North Sea coast in Germany). *Journal Gabeleucht ung und Wasserversorg ung* 44:815–819, 824–844.

Intergovernmental Panel on Climate Change. (2001). *Climate Change 2001: The Scientific Basis*. Edited by J. T. Houghton, Y. Ding, D. J. Griggs, M. Noguer, P. J. van der Linden, X. Dai, K. Maskell and C. A. Johnson. Cambridge, UK.: Cambridge University Press.

Intergovernmental Panel on Climate Change. (2007). *Climate Change 2007: The Physical Science Basis*. Edited by S. Solomon, D. Qin, M. Manning, M. Marquis, K. Averyt, M. M. B. Tignor, H. L. Miller, Jr. and Z. Chen. Cambridge: Cambridge University Press.

Kumar, C. P., A. G. Chacahadi, B. K. Purandara, S. Kumar, and R. Juyal. (2007). Modelling of Seawater Intrusion in Coastal Area of North Goa. *Water Digest* 2 (3):80-83.

Langevin, C.D., Guo, W. (2006). MODFLOW/MT3DMS-based simulation of variable-density groundwater flow and transport. *Ground Water,* 44(3):339-351.

Loáiciga, H. A. (2003). Climate change and ground water. *Annals of the Association of American Geographers* 93 (1):30-41.

Loáiciga, H. A. (2006). Modern-age buildup of CO_2 and its effects on seawater acidity and salinity. *Geophysical Research Letters* 33 (10):L10605 doi:10.1029/2006GL026305.

Loáiciga, H. A. Reply to Comment by Caldeira et al. (2007) on "Modern-age CO_2 and its effect on seawater acidity and salinity". *Geophysical Research Letters*, 34, L18603, doi:10.1029/2006GL027506.

Loáiciga, H. A. (2008). Phreatic surface in island aquifers with regular geometry and time independent recharge and pumping. *Mathematical Geosciences* 40:199-211.

Masterton, J.P., Garabedian, S.P. (2007). Effects of sea-level rise on groundwater flow in a coastal aquifer system. *Ground Water* 45(2):209-217.

Muir, K. S. (1982). Ground Water in the Seaside Area, Monterey County, California: Water-Resources Investigations 82-10, 37: United States Geological Survey.

National Geodetic Survey (NGS). (2009). Continuously Operating Reference Stations. http://www.ngs.noaa.gov/CORS/ (accessed 13 March 2009).

National Oceanic and Atmospheric Administration (NOAA). 2009. Sea Level Trends. http://tidesandcurrents.noaa.gov/sltrends/sltrends.shtml (accessed March 13, 2009).

Panaro, D. 2008. Staff Geologist, Fox Canyon Groundwater Management Agency. Written communication, December, 2008.

Sandwell, D. T. (1987). Biharmonic Spline Interpolation of GOES-3 and SEASAT Altimeter Data. *Geophysical Research Letters* 14 (2):139-142.

Sandoval, Eric. (2008). Written communication, 13 May 2008.

Trefrey, M. G., and C. Muffels. (2007). FEFLOW: A Finite-Element Ground Water Flow and Transport Modeling Tool. *Ground Water* 45 (5):525-528.

United States Geological Survey (USGS). (2008). National Elevation Dataset. http://ned.usgs.gov (accessed 25 February 2008).

United Water Conservation District (UWCD). (1999). Surface and Groundwater Conditions Report: Water Year 1998, 64 p.

Waterloo Hydrogeologic Inc. (2000). Visual Modflow. Waterloo, Ontario, Canada.

Werner, A. D., and C. T. Simmons. (2009). Impact of Sea-Level Rise on Sea Water Intrusion in Coastal Aquifers. *Ground Water* 47 (2):197-204.

Yates, E. B., M. B. Feeney, and L. I. Rosenberg. (2005). Seaside Groundwater Basin: Update on Water Resource Conditions, 47. Monterey, CA: Monterey Peninsula Water Management District.

Yeh, W. W., and B. Bray. (2006). Modeling and Optimization of Seawater Intrusion Barriers in Southern California Coastal Plain, 41: University of California Water Resources Center.

Zekster, I. S., and H. A. Loáiciga. (1993). Groundwater fluxes in the hydrologic cycle: past present and future. *Journal of Hydrology* 144:405-407.

TABLES

Table 1 - Relationship of vertical datums near Seaside, CA (Station ID 9413450, PID GU2090).

Datum	Height (m)
Mean Higher High Water (MHHW)	1.667
Mean High Water (MHW)	1.453
MSL (Mean Sea Level)	0.903
National Geodetic Vertical Datum of 1929 (NGVD29)	0.833
Mean Low Water (MLW)	0.374
Mean Lower Low Water (MLLW)	0.041
North American Vertical Datum of 1988 (NAVD88)	0.000

Table 2 - Relationship of vertical datums near Oxnard, CA (Station ID 9411340, PID EW3742).

Datum	Height (m)
Mean Higher High Water (MHHW)	1.613
Mean High Water (MHW)	1.383
MSL (Mean Sea Level)	0.820
National Geodetic Vertical Datum of 1929 (NGVD29)	0.804
Mean Low Water (MLW)	0.000
Mean Lower Low Water (MLLW)	0.000
North American Vertical Datum of 1988 (NAVD88)	-0.030

LIST OF FIGURES

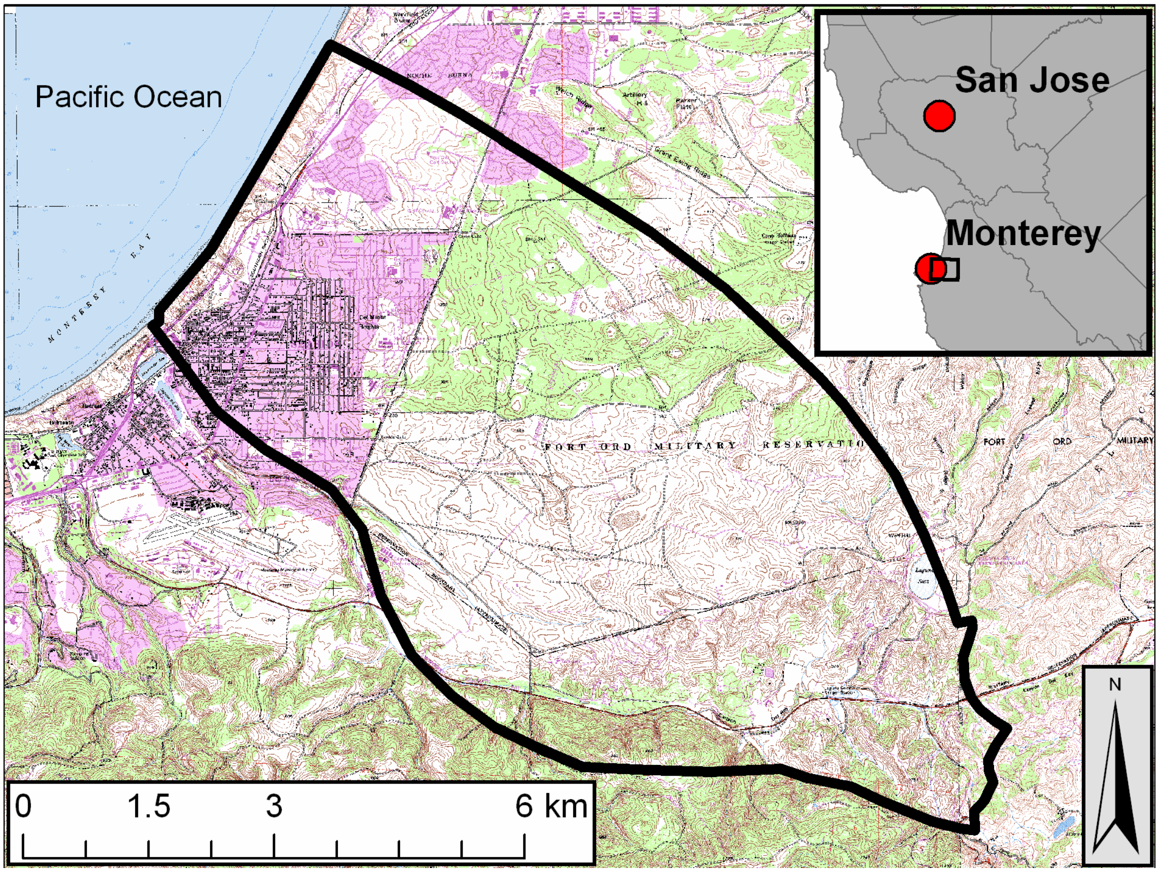

Figure 5 - Seaside Area sub-basin, near Monterey, California.

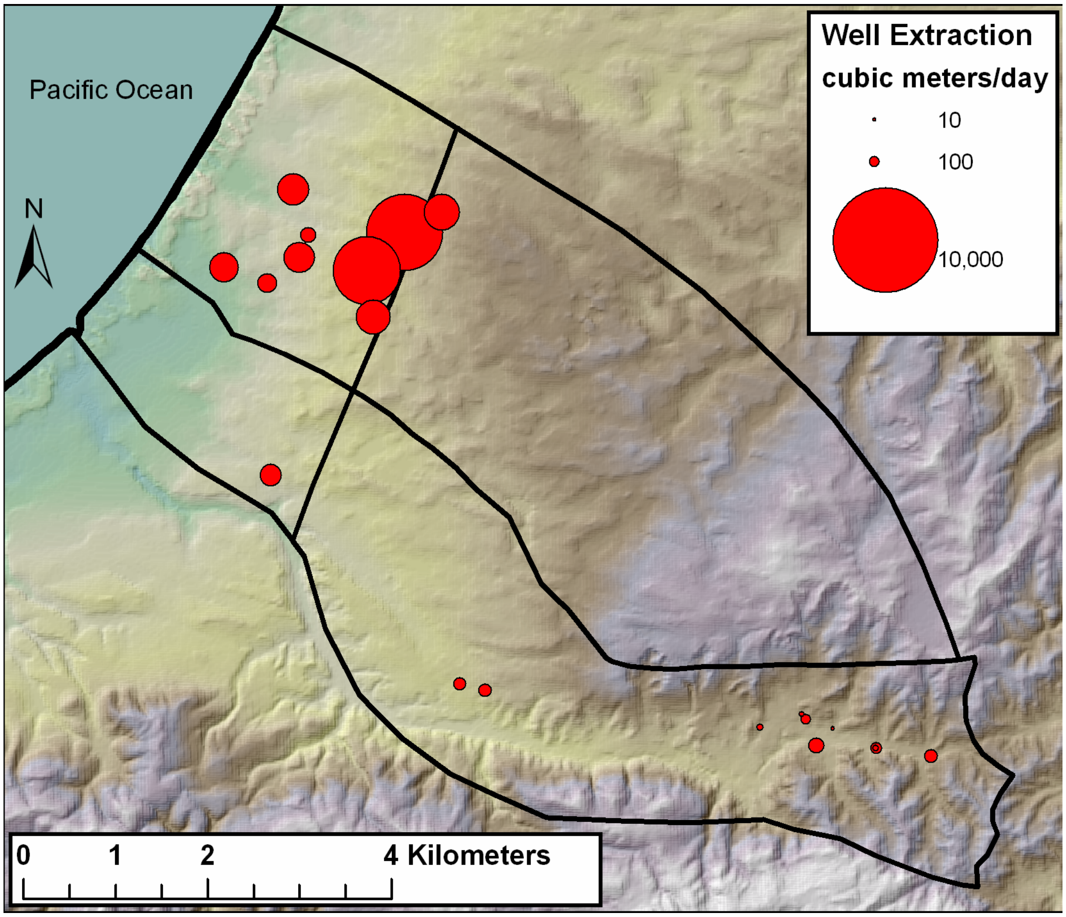

Figure 2 - Proportional circle map of well location and groundwater extractions rates based on information in Yates (2005). The Seaside Area sub-basin is divided into four areas delimited by the black solid lines.

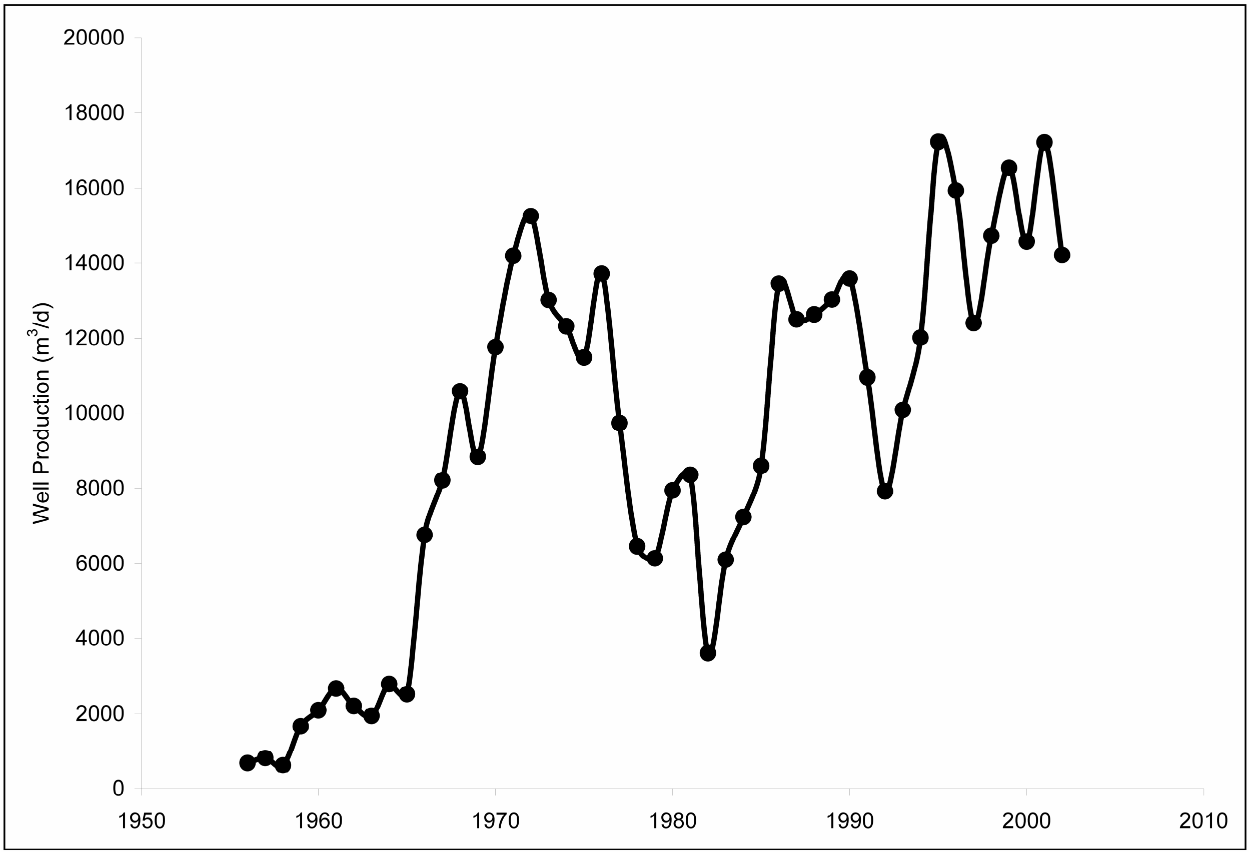

Figure 3 – Groundwater extraction from top fifteen production wells for Seaside Area sub-basin (Durbin, 2007).

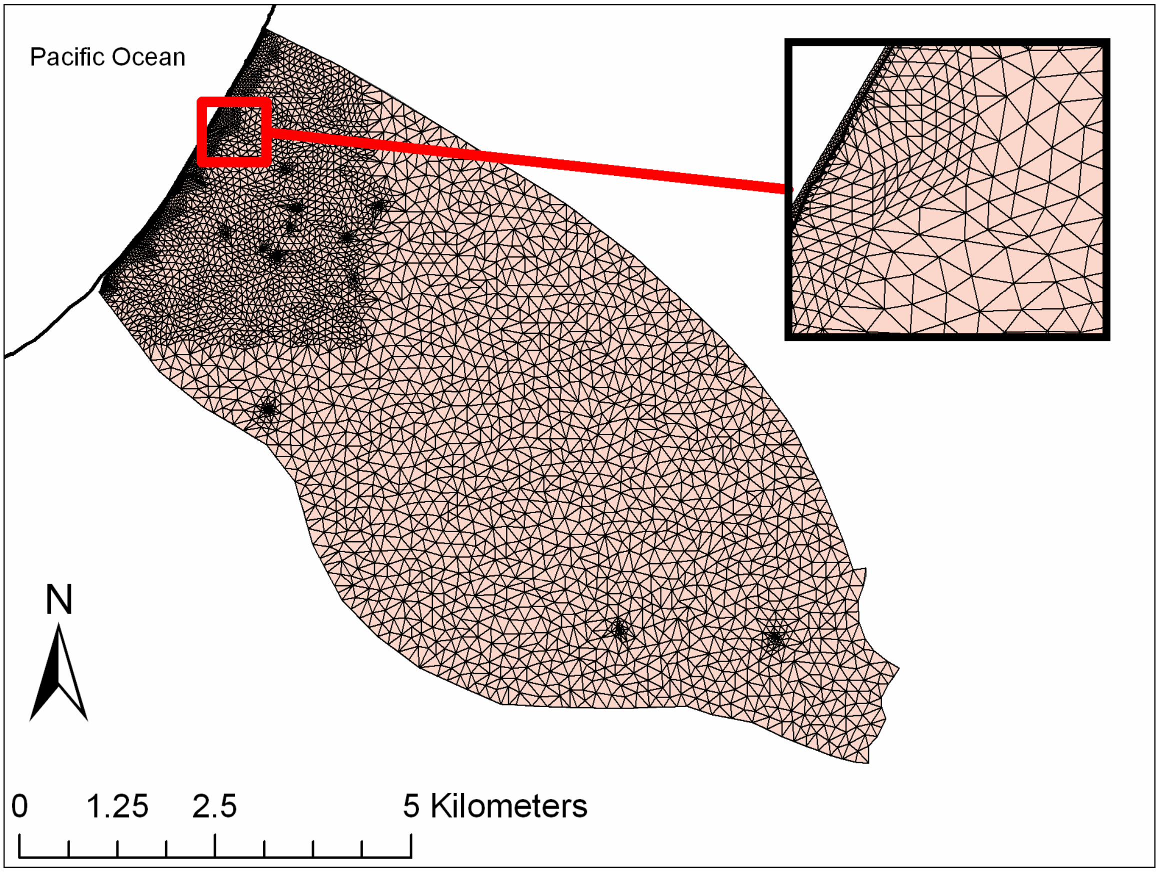

Figure 6 - Triangular finite element mesh for the Seaside Area sub-basin. Notice the finer spatial resolution used near the coastline.

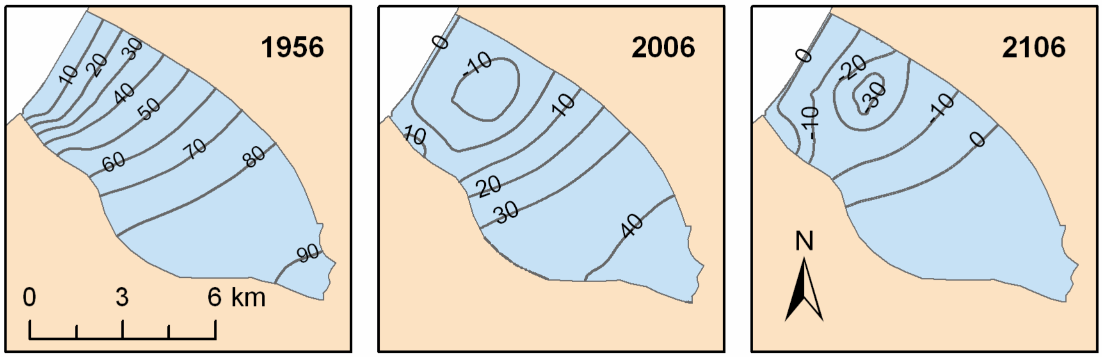

Figure 5 - Simulated hydraulic head distribution (in meters above North American Vertical Datum of 1988) assuming year 2006 net groundwater extraction rates continue to 2106. Sea level was maintained at the 2006 level throughout the simulation. Notice the formation of a cone depression reach -30 m of elevation by 2106.

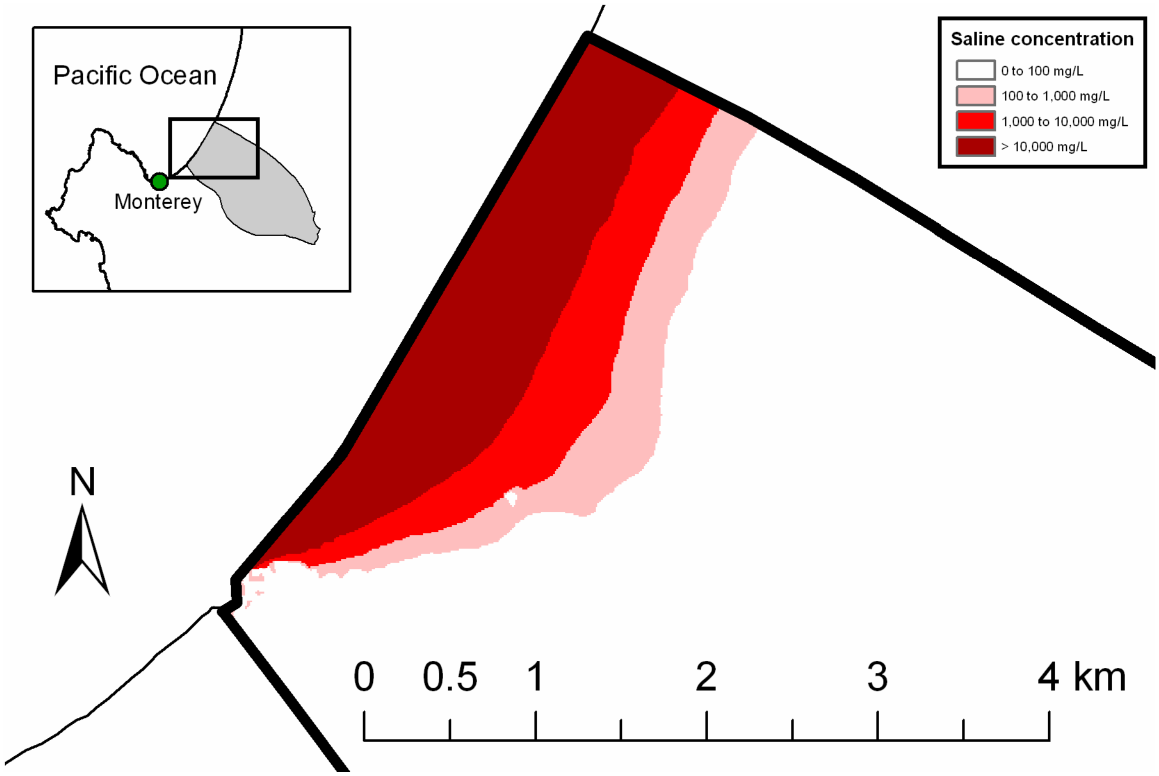

Figure 6 - Saline concentration in the Seaside area sub-basin (California) for year 2106, assuming 1 meter of sea level rise.

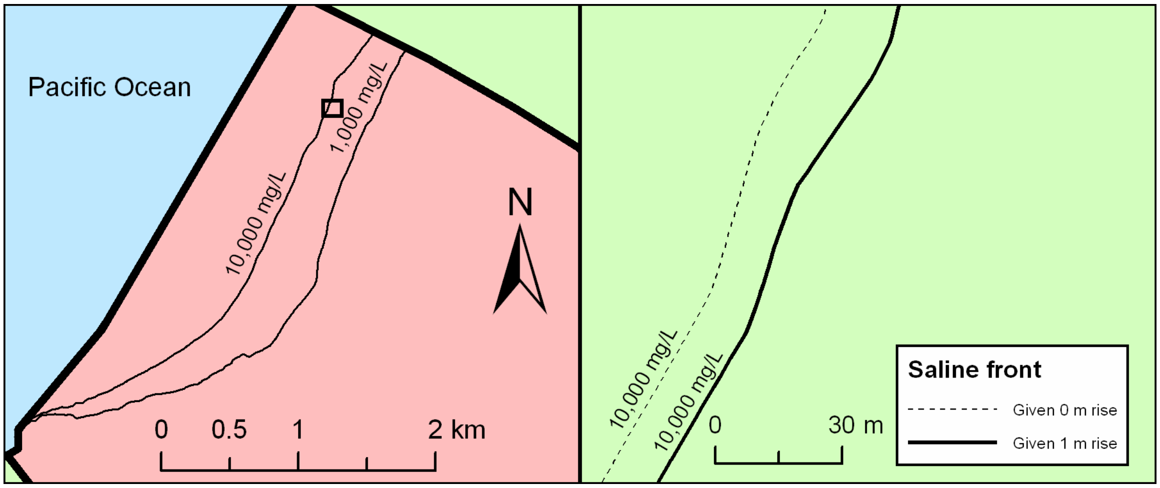

Figure 7 - Effect of sea level rise on saline front intrusion. Left pane illustrates location of the saline isolines for year 2106 assuming 1 meter of sea level rise. The small squared area on the left pane's north-central region is zoomed in on the right pane. The right pane shows the difference between scenarios positing 0 m and 1 m of sea-level rise along the 10,000 mg/L isoline. Notice the iso-concentration lines corresponding to the 0 and 1 m sea-level rises differ in landward advance by about 15 m only.

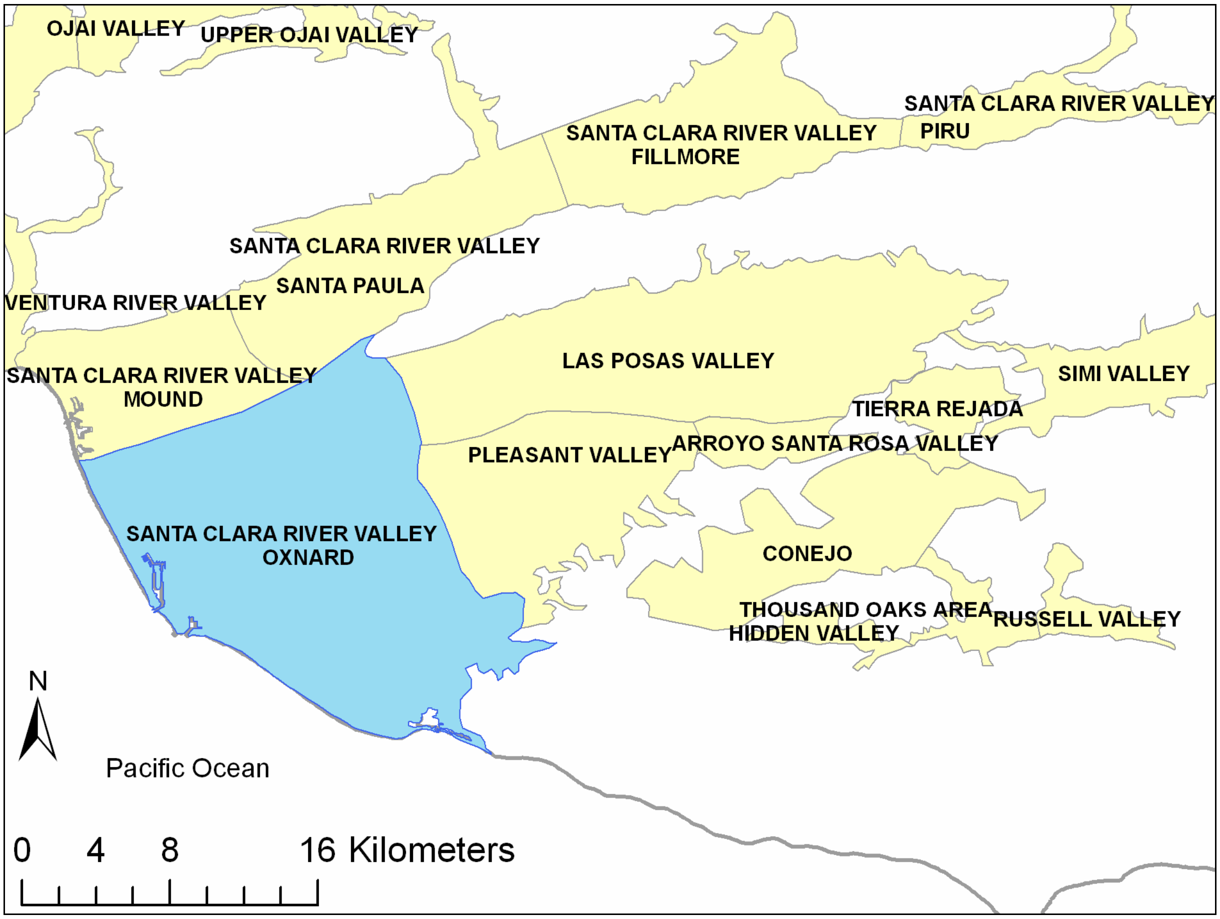

Figure 8 – The Oxnard sub-basin study area in the Santa Clara River Valley groundwater basin (DWR, 2003).

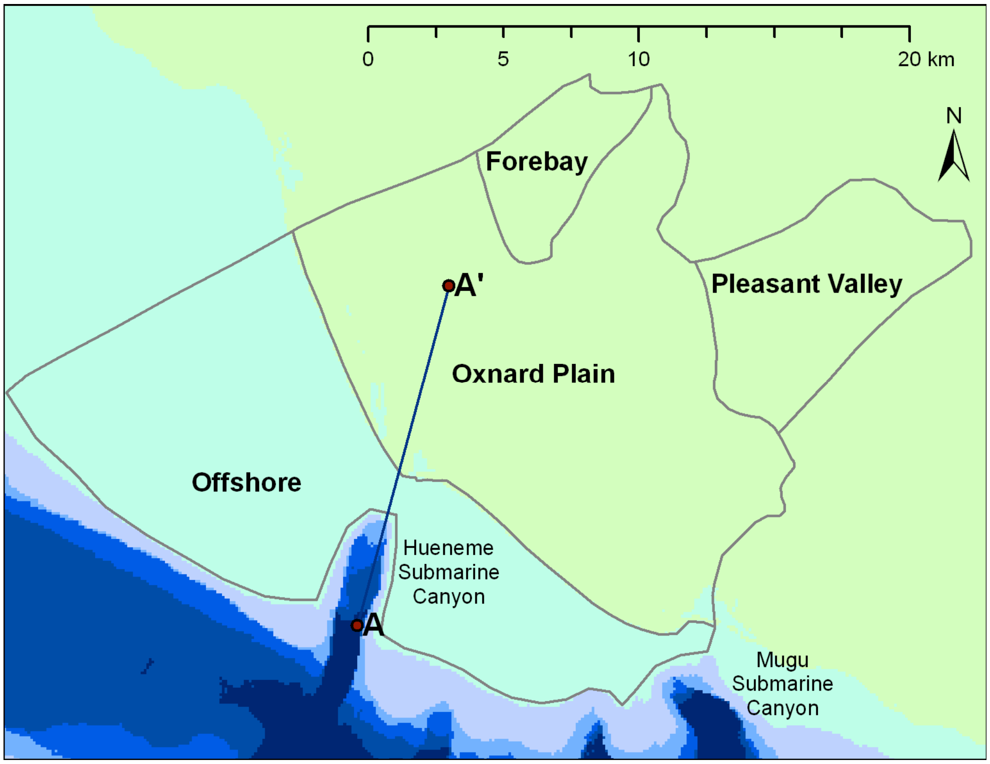

Figure 9 – Boundaries of the Oxnard Plain sub-basin as modeled

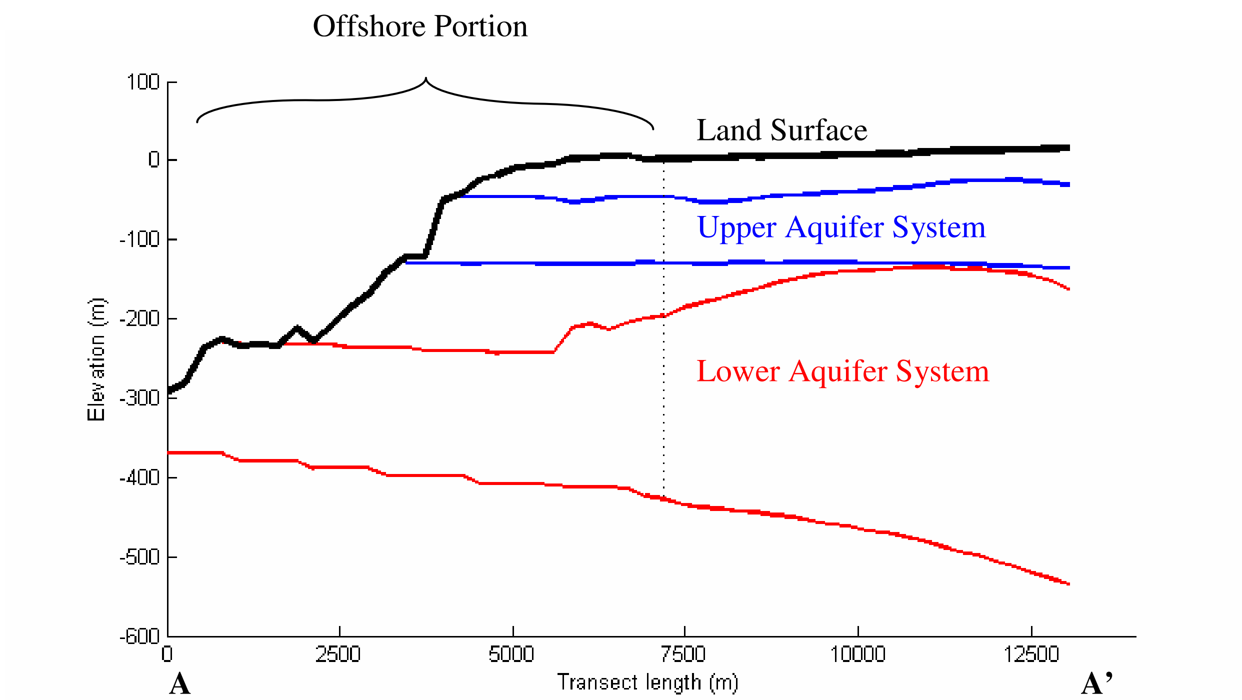

Figure 10 – Transect (A to A') t through the Hueneme Submarine Canyon.